Supporting information

Multi-competitor directed defect engineering in UiO-66: achieving hierarchical porosity and unsaturated sites for high-efficiency fluoroquinolone remediation

Jiawei Kang [a], Fan Qiu [a], Junjie Chen [a], Yaming Wang [a], Yang Fan [a, *], Ying Shen [a], Luqi Guo [a], and Shupeng Zhang [a, *]

[a] *School of Chemistry and Chemical Engineering, Nanjing University of Science and Technology, Nanjing, 210094, PR China*

** Corresponding authors.*

Tel/Fax: +86 25 84315036

E-mail address: fanyangtc9@sina.com; fanyangtc9@njust.edu.cn (Y. Fan)

shupeng_2006@126.com; shupengnjust@njust.edu.cn (S. P. Zhang)

Materials

All of the solvents and reagents were purchased from commercial vendors and used without further purification. Nickel(II) nitrate hexahydrate ($Ni(NO_3)_2·6H_2O$, 98%) and N,N-dimethylformamide (C_3H_7NO, 99%) were purchased from Sinopharm Chemical Reagent Co., Ltd.; Zinc nitrate hexahydrate ($Zn(NO_3)_2·6H_2O$, 99%) was obtained from Xi'an Chemical Reagent Co., Ltd.; Cadmium nitrate tetrahydrate ($Cd(NO_3)_2·4H_2O$, 99%) was purchased from Ron Reagent; Chromium(III) nitrate nonahydrate ($Cr(NO_3)_3·9H_2O$, 99%), sodium sulphate anhydrous (Na_2SO_4, 99%), magnesium chloride hexahydrate ($MgCl_2·6H_2O$, 99%), metronidazole ($C_6H_9N_3O_3$, 99%) and glacial acetic acid ($C_2H_5O_2$, >99.7%) were supplied by Aladdin; Cobalt(II) nitrate hexahydrate ($Co(NO_3)_2·6H_2O$, 99%), sodium chloride (NaCl, 99.5%), rhodamine B ($C_{28}H_{31}ClN_2O_3$, 99%), crystal violet ($C_{25}H_{30}N_3Cl$,90%) and terephthalic acid ($C_8H_6O_4$, 99%) were acquired from Macklin; Iron(III) nitrate nonahydrate ($Fe(NO_3)_3·9H_2O$, >98%) was provided by Nanjing Chemical Reagent Co., Ltd.; Zirconium(IV) chloride ($ZrCl_4$, 98%) was obtained from VOKA. Methylene Blue($C_{16}H_{18}N_3ClS$, ≥98.5%) was obtained from Nanjing Zhongdong Chemical Glass Instrument Co., Ltd. Humic acid was obtained from Shanghai yuanye Bio-Technology Co., Ltd. Levofloxacin ($C_{18}H_{20}FN_3O_4$, 98%) was obtained from Meryer Chemical Technology Co.,Ltd. Tetracycline hydrochloride ($C_{22}H_{24}N_2O_8·HCl$, 98%) was obtained from J&K Scientific.

Characterization

The morphology and elemental distribution of the samples were systematically characterized through scanning electron microscopy (SEM) (JSM-7900F, Japan) and transmission electron microscopy (TEM) (JEM-2100F, Japan), both equipped with energy-dispersive X-ray spectroscopy (EDS) for elemental mapping. X-ray diffraction (XRD) (Bruker D8 Advanced, Germany) was employed to analyze the crystalline structure. The chemical bonding and functional groups were identified using

Fourier transform infrared spectroscopy (FT-IR) (Nicolet IS-10, America) in the wavenumber range of 525-4000 cm^{-1}. Surface charge properties were evaluated by measuring the zeta potential using a dynamic light scattering (DLS) (Malvern Zetasizer Nano ZS90, England) analyzer. The Brunauer-Emmett-Teller (BET) specific surface area and pore size distribution (based on the Barrett-Joyner-Halenda (BJH) model) were determined via N_2 adsorption-desorption isotherms at 77 K (ASAP 3020, America). Thermogravimetric analysis (TGA) (TGA/DSC 3, Switzerland) was conducted from 50 to 800 °C at a heating rate of 10 °C min^{-1} under N_2 atmosphere. The composition and state of elements on the surface of the sample were analyzed by X-ray photoelectron spectroscopy (XPS) (PHI Quantera II, Ulvac-Phi, Japan), test conditions: Al-kα X-ray.

Table S1 Basic information about heterometallic salts.

Serial Number	1	2	3
Molecular Formula	$Mn(NO_3)_2{\cdot}4H_2O$	$Fe(NO_3)_3{\cdot}9H_2O$	$Co(NO_3)_2{\cdot}6H_2O$
Mass/g	0.1004	0.1616	0.1164
Molar Mass/(g/mol)	251.01	404.02	291.03
Serial Number	4	5	6
Molecular Formula	$Ni(NO_3)_2{\cdot}6H_2O$	$Cr(NO_3)_3{\cdot}9H_2O$	$Cd(NO_3)_2{\cdot}4H_2O$
Mass/g	0.1163	0.1601	0.1234
Molar Mass/(g/mol)	290.79	400.15	380.46

Table S2 Basic information of levofloxacin.

Name	Molecular formula	Relative molecular mass	Chemical structural formula	3D chemical structure formula
Levofloxacin	$C_{18}H_{20}FN_3O_4$	361.368	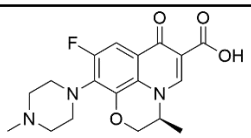	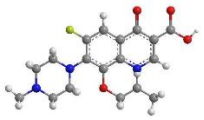

Table S3 Pore structure data on Zr-UiO-66, Zr-UiO-66-D, and Zn/ Zr-UiO-66-D.

Sample	S_1	S_2	S_3	S_{BET}	V_1	V_2	V_{Total}	V_2/V_1	D
Zr-UiO-66	197	36	55	252	0.10	0.03	0.13	0.30	3.87
Zr-UiO-66-D	668	120	185	853	0.35	0.19	0.54	0.54	6.27
Zn/Zr-UiO-66-D	977	135	155	1132	0.50	0.25	0.75	0.50	7.33

Note: S_1 (m^2 g^{-1}) represents the micropore surface area, S_2 (m^2 g^{-1}) denotes the mesopore surface area, S_3 (m^2 g^{-1}) indicates the external surface area (mesopores, macropores, and particle external surface) excluding micropore contributions, and S_{BET} (m^2 g^{-1}) is the BET surface area; V_1 (cm^3 g^{-1}) and V_2 (cm^3 g^{-1}) are the micropore and mesopore volumes, respectively, and V_{Total} (cm^3 g^{-1}) represents the total pore volume; D (nm) is the average pore size.

Table S4 Parameters of different metal competitive species

	Cr^{3+}	Mn^{2+}	Fe^{3+}	Co^{2+}	Ni^{2+}	Zn^{2+}	Zr^{4+}	Cd^{2+}
Atomic Number	24	25	26	27	28	30	40	48
Ionic Radius (Å)	0.62	0.83	0.64	0.74	0.69	0.74	0.72	0.95
Charge Number	3+	2+	3+	2+	2+	2+	4+	2+
Charge Density (e/Å^2)	7.95	2.90	7.19	3.60	4.20	3.65	7.72	2.22
Outer Electron Configuration	$3d^3 4s^0$	$3d^5 4s^0$	$3d^5 4s^0$	$3d^7 4s^0$	$3d^8 4s^0$	$3d^{10} 4s^0$	$4d^0 5s^0$	$4d^{10} 5s^0$
Hydrolysis Constant	4.0	10.6	2.2	9.6	9.9	9.0	<0	10.1

Note: The charge density (e/Å^2) was calculated as the charge number divided by the square of the ionic radius [1]. The hydrolysis constant (pK_h) represents the first-stage hydrolysis constant [2], where a lower value indicates greater ease of metal ion hydrolysis, leading to increased competition with ligands for coordination and consequently reduced coordination capability.

Table S5 Pore structure data on Zn/ Zr-UiO-66-DT and Zn/Zr-UiO-66-D.

Sample	Zn/Zr-UiO-66-DT	Zn/Zr-UiO-66-D
S_1[a](m^2/g)	814	977
S_2[b](m^2/g)	178	135
S_3[c](m^2/g)	240	155
S_{BET}[d](m^2/g)	1,054	1132
V_1[e](cm^3/g)	0.42	0.50
V_2[f](cm^3/g)	0.39	0.25
V_{Total}[g](cm^3/g)	0.81	0.75
V_2/V_1	0.93	0.50
D[h](nm)	8.73	7.33

[a] Micropore surface area. [b] Mesopore surface area. [c] External surface area (mesopores, macropores, and particle external surface) excluding micropore contributions. [d] BET surface area; [e] Micropore volumes. [f] Mesopore volumes. [g] Total pore volume. [h] Average pore size.

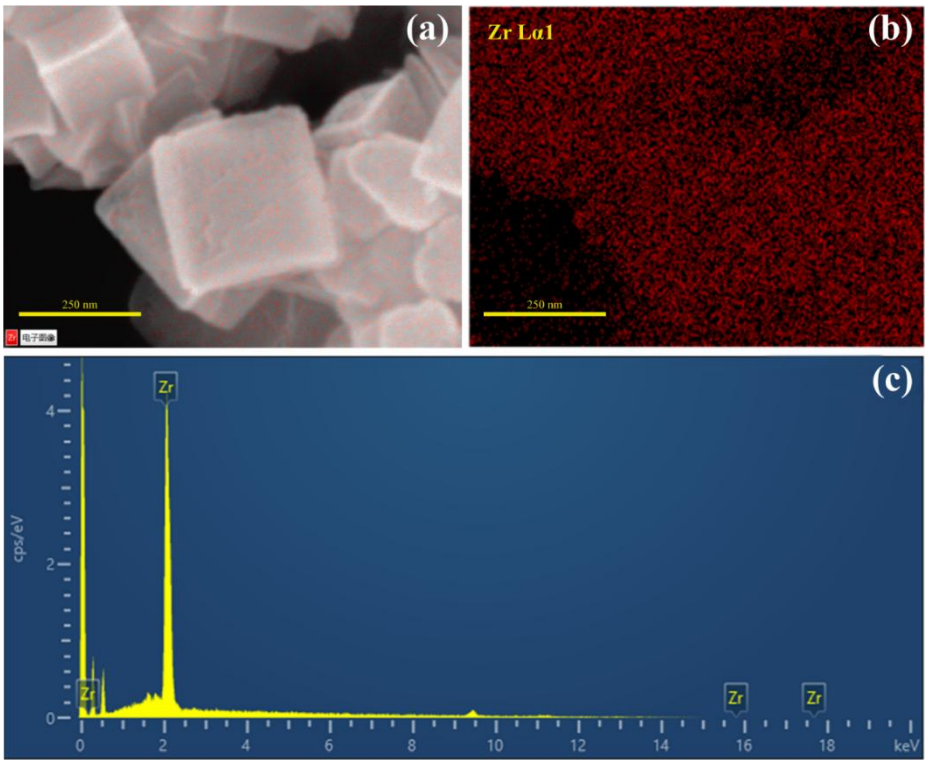

Fig. S1 SEM image (a), elemental mapping (Zr Lα1) (b) and EDX spectrum of Zr-UiO-66 (c).

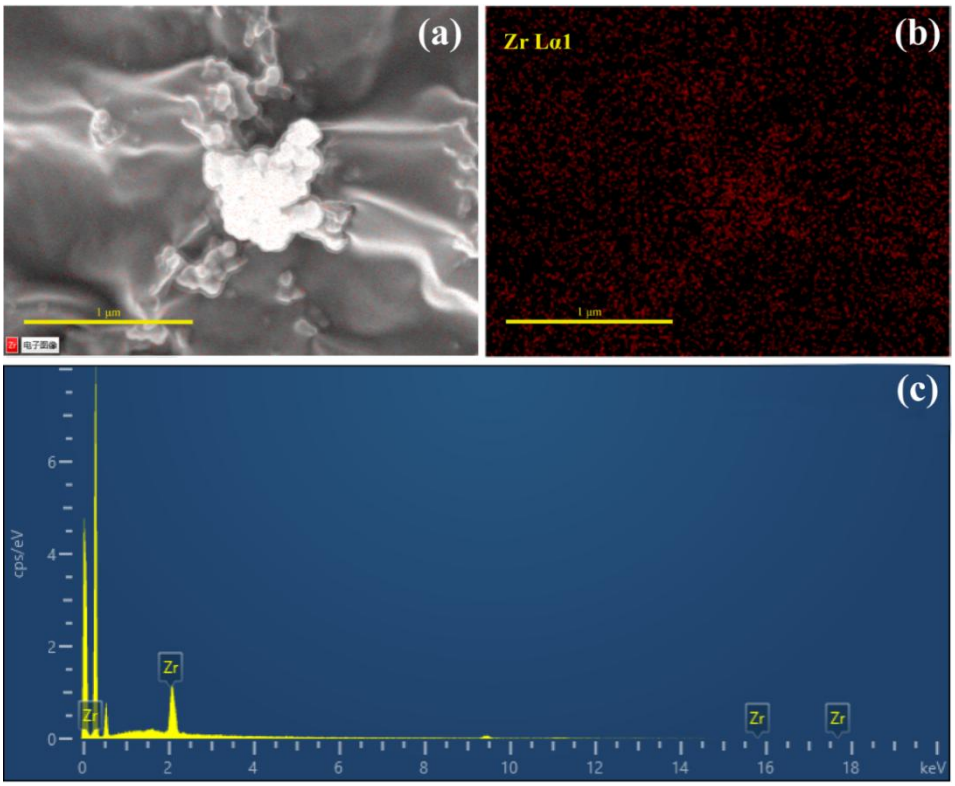

Fig. S2 SEM image (a), elemental mapping (Zr Lα1) (b) and EDX spectrum of Zr-UiO-66-D (c).

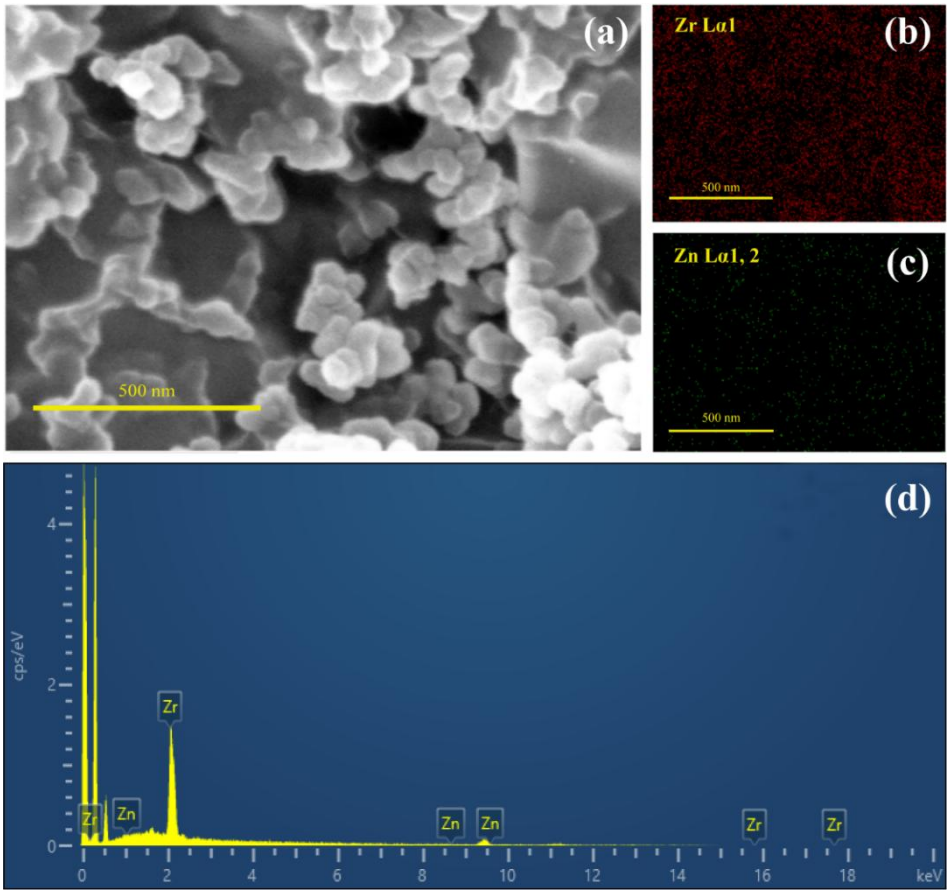

Fig. S3 SEM image (a), elemental mapping (Zr Lα1 (b), Zn Lα1, 2 (c)) and EDX spectrum of Zn/Zr-UiO-66-D (d).

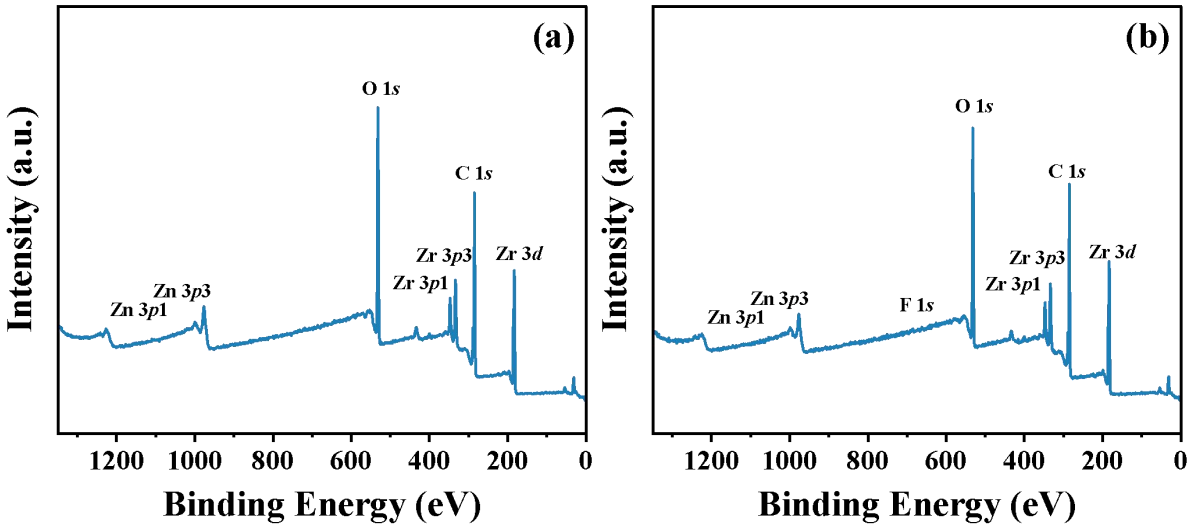

Fig. S4 XPS survey spectra of Zn/Zr-UiO-66-D before (a) and after (b) LVX adsorption

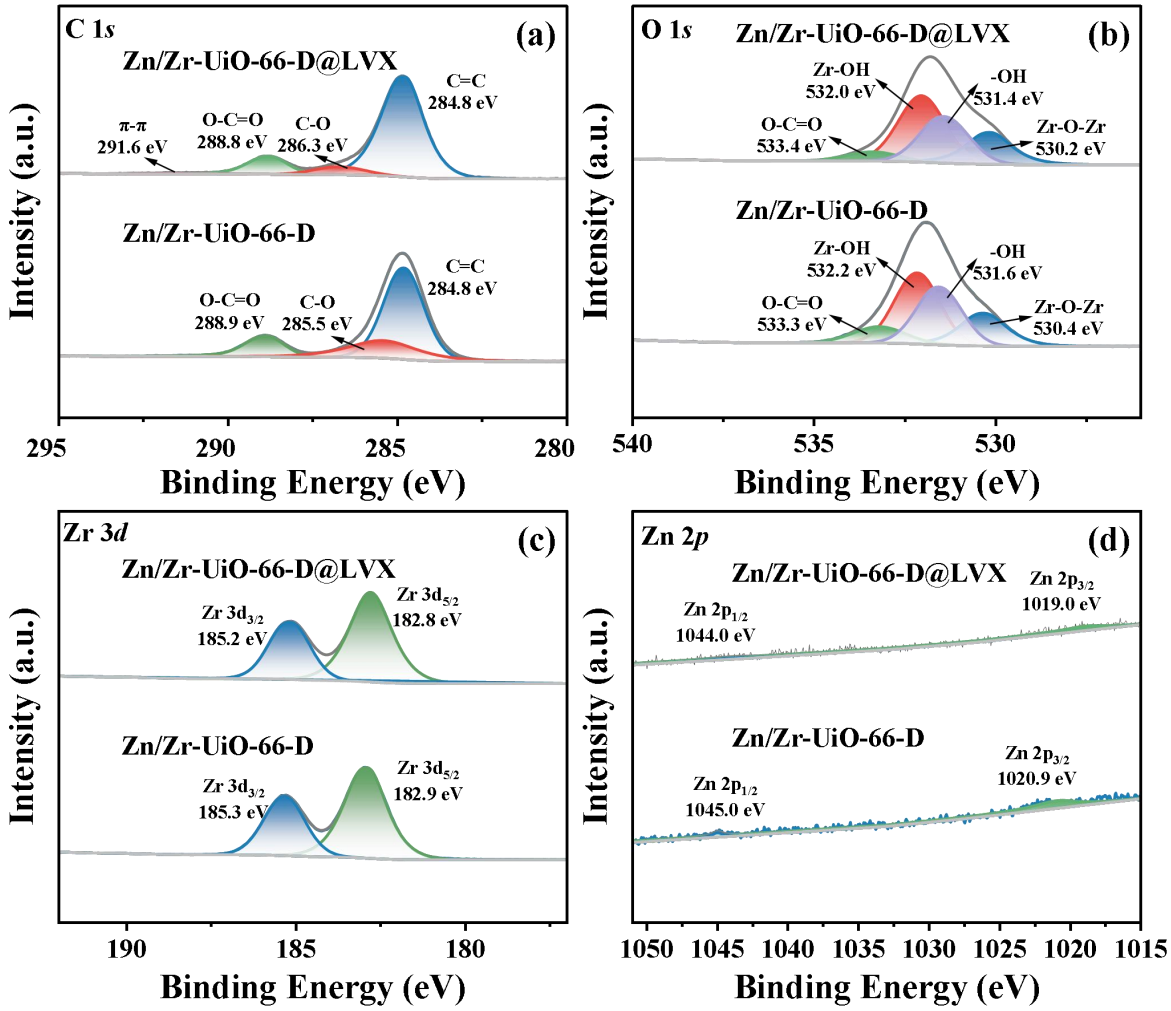

Fig. S5 High-resolution XPS spectra of Zn/Zr-UiO-66-D before and after levofloxacin (LVX) adsorption: (a) C 1s, (b) O 1s, (c) Zr 3d, (d) Zn 2p

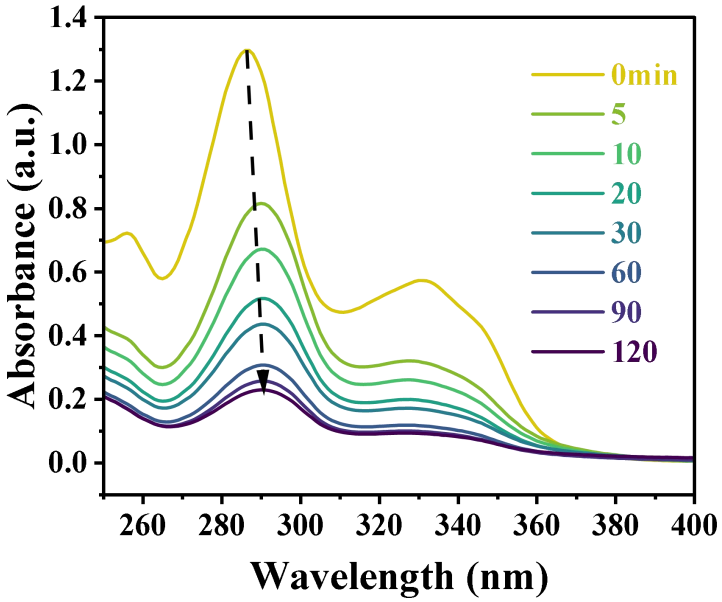

Fig. S6 Adsorption of LVX by Zn/Zr-UiO-66-DT (as indicated by the time-dependent absorbance changes of LVX in aqueous solution).

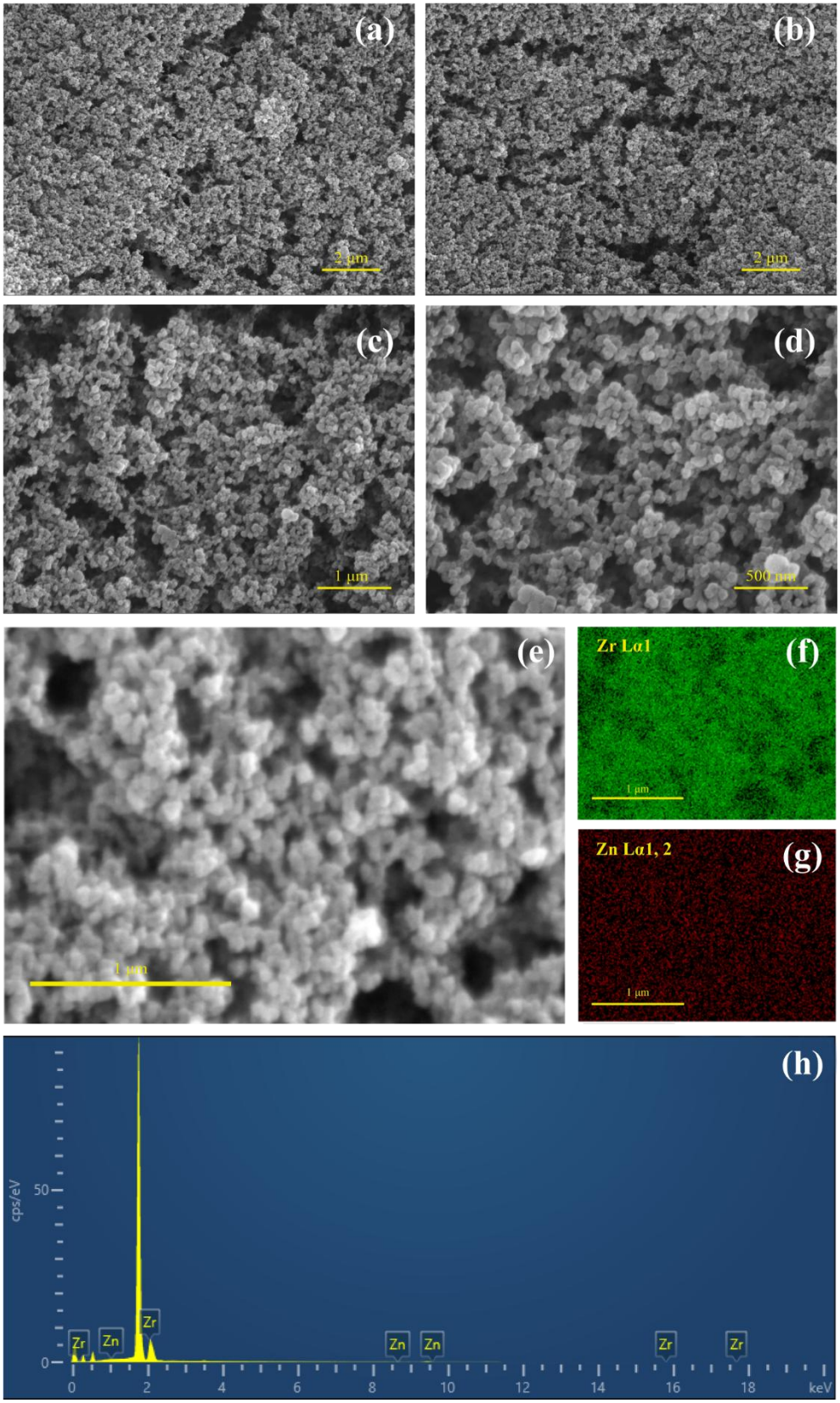

Fig. S7 SEM image at different magnifications (a-e), elemental mapping (Zr Lα1 (f), Zn Lα1, 2 (g)) and EDX spectrum of Zn/Zr-UiO-66-D (h).

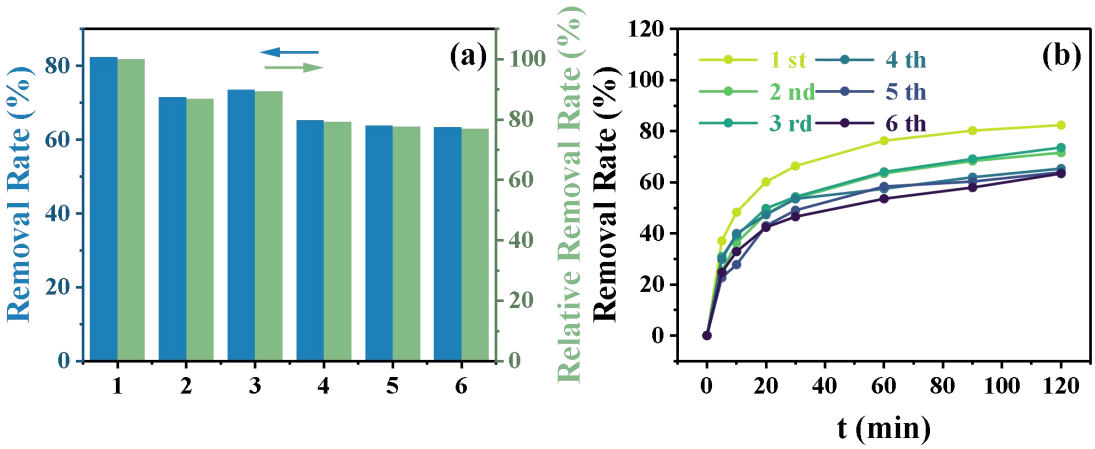

Fig. S8 Cycle-dependent removal efficiency (blue bars) and relative removal efficiency (green bars, defined as the ratio of LVX removal efficiency in each cycle to that in the first cycle) of Zn/Zr-UiO-66-DT through six consecutive adsorption-desorption cycles (a). Time-dependent LVX removal profiles for each regeneration cycle (b).

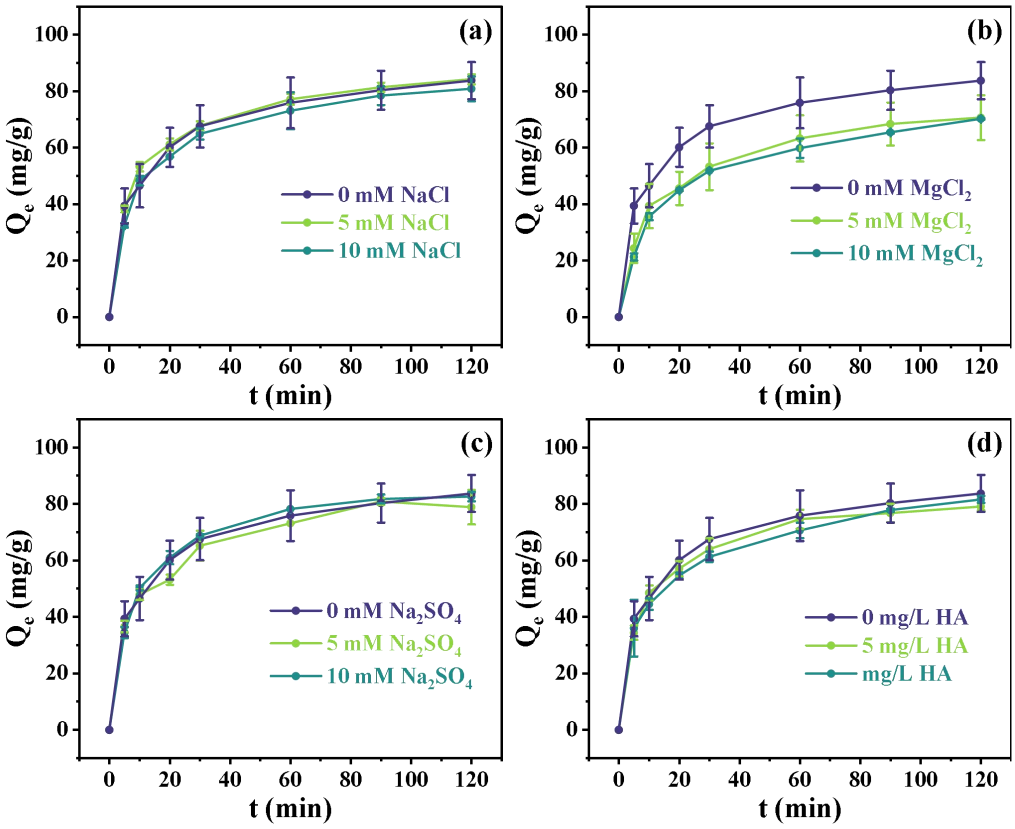

Fig. S9 Time-dependent adsorption quantities of Zn/Zr-UiO-66-DT toward LVX under varying concentrations (0, 5, 10 mM) of NaCl (a), $MgCl_2$ (b), Na_2SO_4 (c), and humic acid (HA) (d).

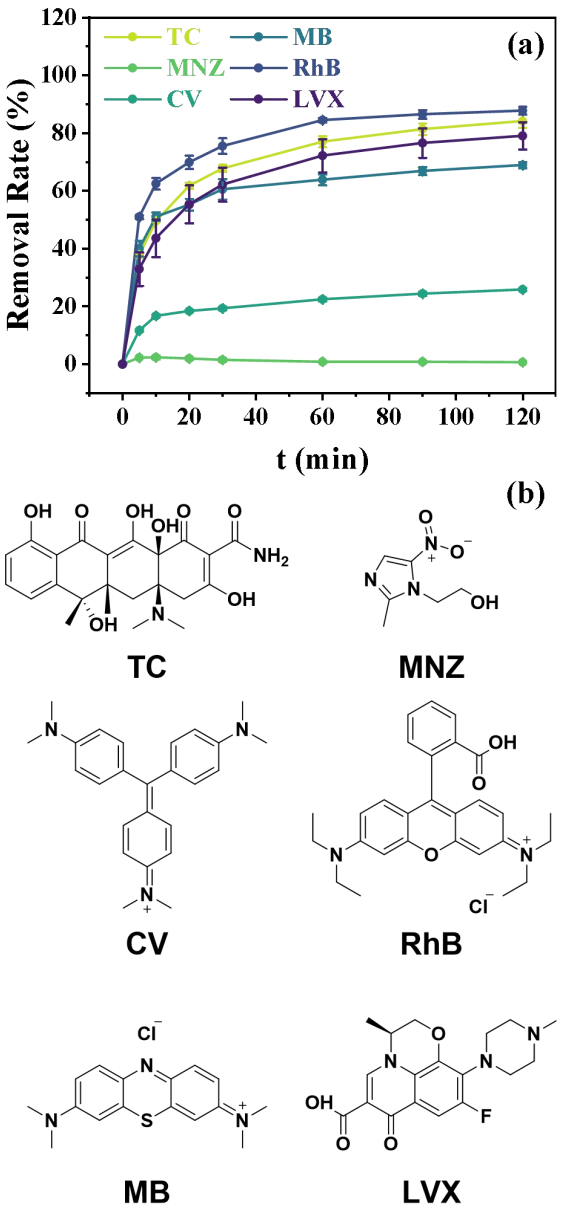

Fig. S10 Time-dependent adsorption capacities of Zn/Zr-UiO-66-DT toward TC, MNZ, CV, RhB, MB and LVX (a). Structural formulas of TC, MNZ, CV, RhB, MB and LVX (b).

References:

1. Shannon, R. D., Revised effective ionic radii and systematic studies of interatomic distances in halides and chalcogenides. *Acta Crystallographica Section A* 1976, **32**, (5), 751-767.

2. Barnum, D. W., Hydrolysis of cations. Formation constants and standard free energies of formation of hydroxy complexes. *Inorg. Chem.* 1983, **22**, (16), 2297-2305.